Journal of Nuclear Materials 393 (2009) 465–472

Contents lists available at ScienceDirect

Journal of Nuclear Materials

journal homepage: www.elsevier.com/locate/jnucmat

# Photon interaction and energy absorption in glass: A transparent gamma ray shield

S.R. Manohara [a], S.M. Hanagodimath [a], L. Gerward [b,*]

[a] Department of Physics, Gulbarga University, Gulbarga 585 106, Karnataka, India
[b] Department of Physics, Technical University of Denmark, DK-2800 Lyngby, Denmark

ARTICLE INFO

*Article history:*
Received 16 October 2008
Accepted 6 July 2009

*PACS:*
33.80.−b
78.70.−g
81.05.Kf

ABSTRACT

The effective atomic number, $Z_{eff}$, the effective electron density, $N_{e,eff}$, and the energy dependence, *ED*, have been calculated at photon energies from 1 keV to 1 GeV for CaO–SrO–$B_2O_3$, PbO–$B_2O_3$, $Bi_2O_3$–$B_2O_3$, and PbO–$Bi_2O_3$–$B_2O_3$ glasses with potential applications as gamma ray shielding materials. For medium-*Z* glasses, $Z_{eff}$ is about constant and equal to the mean atomic number in a wide energy range, typically $0.3 < E < 4$ MeV, where Compton scattering is the main photon interaction process. In contrast, for high-*Z* glasses there is no energy region where Compton scattering is truly dominating. Heavy-metal oxide glasses containing PbO and/or $Bi_2O_3$ are promising gamma ray shielding materials due to their high effective atomic number and strong absorption of gamma rays. They compare well with concrete and other standard shielding materials and have the additional advantage of being transparent to visible light. The single-valued effective atomic number calculated by XMuDat is approximately valid at low energies where photoelectric absorption is dominating.



## 1. Introduction

The interaction of high-energy photons with matter is important in radiation medicine and biology, nuclear engineering, and space technology. Glass has the double function of being transparent to visible light and absorbing gamma rays and neutrons, thus providing a radiation shield for observers or experimenters. It may also be mentioned that vitrification is an interesting option for long-term storage of radioactive waste products.

The effective atomic number, $Z_{eff}$, and the effective electron density, $N_{e,eff}$, are in some cases convenient parameters for characterizing scattering and absorption of gamma rays in a given material. For example, the effective atomic number can be used when estimating the chemical composition of an unknown compound, or when substituting a chemical element for a complex material [1]. It should be noted, however, that the atomic numbers of the constituent elements of the material have to be weighted differently for each of the different processes, by which gamma radiation can interact with matter. Therefore, the effective atomic number of a given material is not constant. It is varying with photon energy depending on the interaction processes involved.

Early calculations of effective atomic numbers were based on parameterization of the photon interaction cross-section by fitting data over limited ranges of photon energy and atomic number [2]. Today, accurate databases of photon interaction cross-sections and interpolation programs [3–5] have made it possible to calculate effective atomic numbers with much improved accuracy and information content over wide ranges of photon energy and elemental composition. In a previous work [6] we have derived a comprehensive and consistent set of formulas for calculating the effective atomic number. These formulas are valid for all types of materials and for all energies above 1 keV, far into the GeV range.

There is an increasing interest in heavy-metal oxide (HMO) glasses, based on for example PbO or $Bi_2O_3$, because of their good gamma ray shielding properties [7–11]. However, a high lead content lowers the melting point and the hardness of the glass. Moreover, it is desirable to replace lead with other elements because of environmental considerations. Recently, bismuth based glass have received attention due to its many potential applications [12,13]. Boric oxide, $B_2O_3$, is added mainly for increasing the melting point and the ability to withstand high temperatures.

Several authors have measured absorption coefficients, effective atomic numbers or effective electron densities of glasses at energies around 1 MeV [7–11,14–17], but there are almost no studies at lower and higher energies. In the present work, we have calculated the effective atomic number and related parameters at photon energies from 1 keV to 1 GeV for CaO–SrO–$B_2O_3$, PbO–$B_2O_3$, $Bi_2O_3$–$B_2O_3$, and PbO–$Bi_2O_3$–$B_2O_3$ glasses using photon interaction cross-sections from the WinXCom interpolation program [3,4] and

* Corresponding author.
*E-mail address:* gerward@fysik.dtu.dk (L. Gerward).

0022-3115/$ - see front matter © 2009 Elsevier B.V. All rights reserved.
doi:10.1016/j.jnucmat.2009.07.001

the NIST database [5]. Wherever possible, the calculations are compared with experimental data. We are also comparing the glasses with standard radiation shielding materials, such as concrete. Finally, we are discussing the single-valued effective atomic number and electron density provided by the program XMuDat [18].

## 2. Calculations of effective atomic number, $Z_{eff}$, effective electron density, $N_{e,eff}$, and energy dependence, ED

In practical work, the effective atomic number for photon interaction, $Z_{PI,eff}$, can be calculated from the following formula [6]:

$$Z_{PI,eff} = \frac{\sum_i f_i A_i \left(\frac{\mu}{\rho}\right)_i}{\sum_j f_j \frac{A_j}{Z_j} \left(\frac{\mu}{\rho}\right)_j} \quad (1)$$

where $f_i$ is the molar fraction of the $i$th constituent element (normalized so that $\sum_i f_i = 1$), $A_i$ is the atomic mass, $Z_i$ is the atomic number, and $(\mu/\rho)_i$ is the mass attenuation coefficient. WinXCom [4,5] has been used for calculating the mass attenuation coefficients. Each one of the glasses considered is a mixture of CaO, SrO, PbO, $Bi_2O_3$, and $B_2O_3$ in various proportions. The ability of WinXCom to calculate mass attenuation coefficients for mixtures of compounds is therefore very useful.

The effective atomic number for photon energy absorption, $Z_{PEA,eff}$, is obtained from Eq. (1) by substituting the mass energy-absorption coefficient, $\mu_{en}/\rho$, for the mass attenuation coefficient, $\mu/\rho$. Mass energy-absorption coefficients have been obtained from the tabulation of Hubbell and Seltzer [19].

The effective electron density, $N_{e,eff}$, expressed in number of electrons per unit mass, is closely related to the effective atomic number and given by

$$N_{e,eff} = N_A \frac{Z_{eff}}{\sum_i f_i A_i} = N_A \frac{Z_{eff}}{\langle A \rangle} \quad (2)$$

where $N_A$ is the Avogadro constant, and $\langle A \rangle = \sum_i f_i A_i$ is the average atomic mass of the material.

Similarly, the average electron density can be written

$$\langle N_e \rangle = N_A \frac{\sum_i f_i Z_i}{\sum_j f_j A_j} = N_A \frac{\langle Z \rangle}{\langle A \rangle} \quad (3)$$

where $\langle Z \rangle = \sum_i f_i Z_i$ is the mean atomic number of the material. The average electron density is readily calculated from the chemical composition and the Avogadro constant. Moreover, for low- and medium-$Z$ elements, the ratio $Z/A$ is nearly ½. Hence, according to Eq. (3), $\langle N_e \rangle$ is approximately one-half Avogadro's number, or about $3 \times 10^{23}$ electrons/g.

The energy dependence, $ED$, is defined as the ratio between the mass energy-absorption coefficient of the material under consideration and the mass energy-absorption coefficient of air [20]:

$$ED = \frac{(\mu_{en}/\rho)_{Glass}}{(\mu_{en}/\rho)_{Air}} \quad (4)$$

XMuDat [18] is another program for presentation and calculation of absorption coefficients and related parameters in the energy range from 1 keV to 50 MeV. For a given compound or mixture the program also provides a single-valued effective atomic number, which in the following will be called $Z_{X,eff}$. It is calculated according to the formula:

$$Z_{X,eff} = \left( \sum_i \alpha_i Z_i^{m-1} \right)^{1/(m-1)} \quad (5)$$

**Table 1**
Chemical composition of glasses studied in the present work. S.N. = sample number, $\langle Z \rangle$ = mean atomic number. $Z_{PI,eff}$ and $Z_{PEA,eff}$ are the effective atomic numbers for photon interaction and for energy absorption, respectively. Maximum and minimum values are given for the energy range considered (1 keV–1 GeV). $Z_{X,eff}$ is the single-valued effective atomic number provided by XMuDat [18].

| S.N | Composition (mole fraction) | | | | | $\langle Z \rangle$ | $Z_{PI,eff}$ | | $Z_{X,eff}$ | $Z_{PEA,eff}$ | |
|---|---|---|---|---|---|---|---|---|---|---|---|
| | CaO | SrO | PbO | $Bi_2O_3$ | $B_2O_3$ | | Max | Min | | Max | Min |
| 1 | 0.00 | 0.30 | – | – | 0.70 | 9.17 | 34.95 | 9.23 | 27.08 | 35.65 | 9.18 |
| 2 | 0.05 | 0.25 | – | – | 0.70 | 8.95 | 33.94 | 9.00 | 25.98 | 34.74 | 8.96 |
| 3 | 0.10 | 0.20 | – | – | 0.70 | 8.73 | 32.61 | 8.77 | 24.68 | 33.52 | 8.74 |
| 4 | 0.15 | 0.15 | – | – | 0.70 | 8.51 | 30.77 | 8.54 | 23.09 | 31.80 | 8.51 |
| 5 | 0.20 | 0.10 | – | – | 0.70 | 8.29 | 28.07 | 8.31 | 21.06 | 29.22 | 8.29 |
| 6 | 0.25 | 0.05 | – | – | 0.70 | 8.07 | 23.69 | 8.09 | 18.20 | 24.88 | 8.07 |
| 7 | 0.30 | 0.00 | – | – | 0.70 | 7.85 | 15.48 | 7.86 | 12.84 | 16.32 | 7.85 |
| 8 | – | – | 0.10 | – | 0.90 | 8.43 | 66.30 | 8.85 | 52.29 | 71.48 | 8.84 |
| 9 | – | – | 0.20 | – | 0.80 | 10.27 | 73.83 | 11.15 | 61.38 | 76.75 | 11.14 |
| 10 | – | – | 0.30 | – | 0.70 | 12.39 | 76.79 | 13.75 | 66.65 | 78.71 | 13.73 |
| 11 | – | – | 0.40 | – | 0.60 | 14.84 | 78.38 | 16.71 | 70.23 | 79.73 | 16.69 |
| 12 | – | – | 0.50 | – | 0.50 | 17.71 | 79.36 | 20.12 | 72.86 | 80.35 | 20.09 |
| 13 | – | – | 0.60 | – | 0.40 | 21.13 | 80.03 | 24.08 | 74.88 | 80.78 | 24.04 |
| 14 | – | – | 0.70 | – | 0.30 | 25.24 | 80.52 | 28.73 | 76.49 | 81.08 | 28.69 |
| 15 | – | – | 0.80 | – | 0.20 | 30.31 | 80.89 | 34.29 | 77.58 | 81.31 | 34.25 |
| 16 | – | – | 0.90 | – | 0.10 | 36.70 | 81.18 | 41.04 | 78.91 | 81.49 | 40.99 |
| 17 | – | – | – | 0.10 | 0.90 | 9.92 | 73.88 | 10.74 | 60.72 | 77.13 | 10.73 |
| 18 | – | – | – | 0.20 | 0.80 | 13.04 | 78.23 | 14.59 | 68.45 | 80.00 | 14.58 |
| 19 | – | – | – | 0.30 | 0.70 | 16.16 | 79.81 | 18.36 | 72.28 | 81.01 | 18.34 |
| 20 | – | – | – | 0.40 | 0.60 | 19.28 | 80.62 | 22.05 | 74.61 | 81.52 | 22.02 |
| 21 | – | – | – | 0.50 | 0.50 | 22.40 | 81.12 | 25.65 | 76.19 | 81.83 | 25.62 |
| 22 | – | – | – | 0.60 | 0.40 | 25.52 | 81.46 | 29.18 | 77.33 | 82.04 | 29.14 |
| 23 | – | – | – | 0.70 | 0.30 | 28.64 | 81.70 | 32.64 | 78.19 | 82.20 | 32.59 |
| 24 | – | – | – | 0.80 | 0.20 | 31.76 | 81.88 | 36.02 | 78.87 | 82.31 | 35.97 |
| 25 | – | – | – | 0.90 | 0.10 | 34.88 | 82.03 | 39.33 | 79.41 | 82.40 | 39.29 |
| 26 | – | – | 0.05 | 0.10 | 0.85 | 10.80 | 75.56 | 11.83 | 63.51 | 78.19 | 11.82 |
| 27 | – | – | 0.10 | 0.20 | 0.70 | 15.06 | 79.20 | 17.03 | 71.04 | 80.55 | 17.01 |
| 28 | – | – | 0.15 | 0.30 | 0.55 | 19.60 | 80.51 | 22.41 | 74.67 | 81.38 | 22.38 |
| 29 | – | – | 0.20 | 0.40 | 0.40 | 24.45 | 81.18 | 27.96 | 76.83 | 81.80 | 27.92 |
| 30 | – | – | 0.25 | 0.50 | 0.25 | 29.65 | 81.59 | 33.71 | 78.28 | 82.05 | 33.66 |
| 31 | – | – | 0.30 | 0.60 | 0.10 | 35.22 | 81.86 | 39.66 | 79.32 | 82.22 | 39.61 |

where $\alpha_i$ is the fractional number of electrons of element $i$, and $m$ is a constant between 3 and 5. It is suggested that $m$ is set to 3.6 for materials with $Z_{eff} < 6$, and 4.1 for a material with $Z_{eff}$ higher than 6 [2]. In addition, XMuDat provides an electron density that will be discussed below in Section 3.3.

## 3. Results and discussion

The composition of the glasses studied in the present work is given in Table 1 together with the corresponding values of the mean atomic number, and the maximum and minimum values of the effective atomic number in the photon energy range from 1 keV to 1 GeV. In the following, one composition of each type of glass has been chosen for a detailed discussion.

### 3.1. $CaO–SrO–B_2O_3$

Fig. 1a shows the effective atomic number (for photon interaction) as a function of energy for a sample with composition 15CaO–15SrO–70$B_2O_3$ (sample #4). The energy behavior of the effective

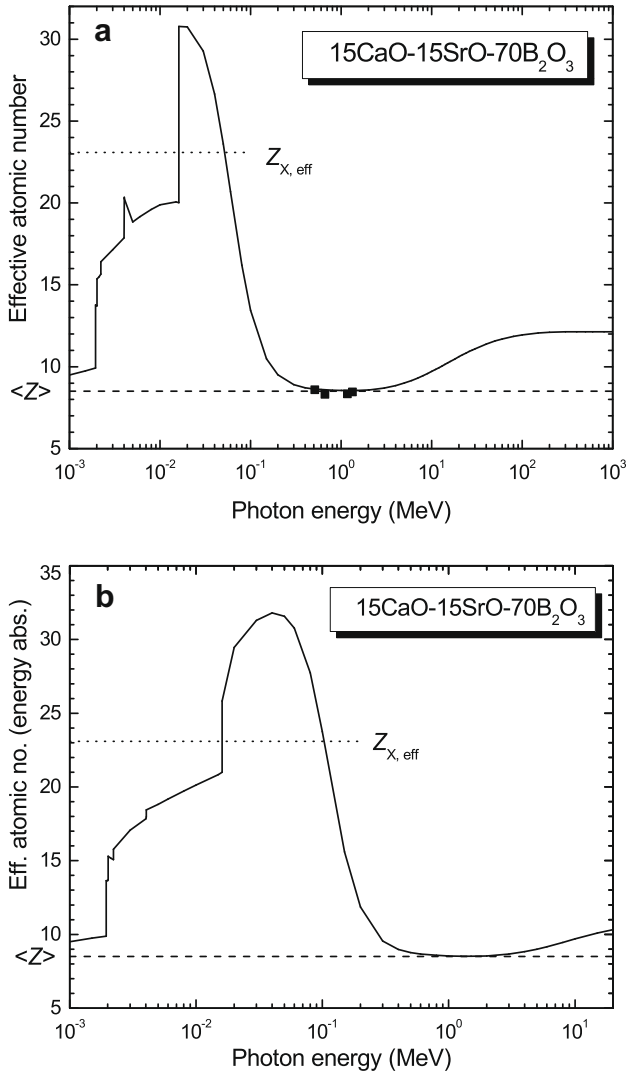


**Fig. 1.** The effective atomic number of 15CaO–15SrO–70$B_2O_3$ as a function of photon energy. The dashed line indicates the mean atomic number, $\langle Z \rangle$, and the dotted line the single-valued effective atomic number, $Z_{X,eff}$, provided by XMuDat. (a) Photon interaction. The squares are experimental data points of Singh et al. [17]. (b) Energy absorption.

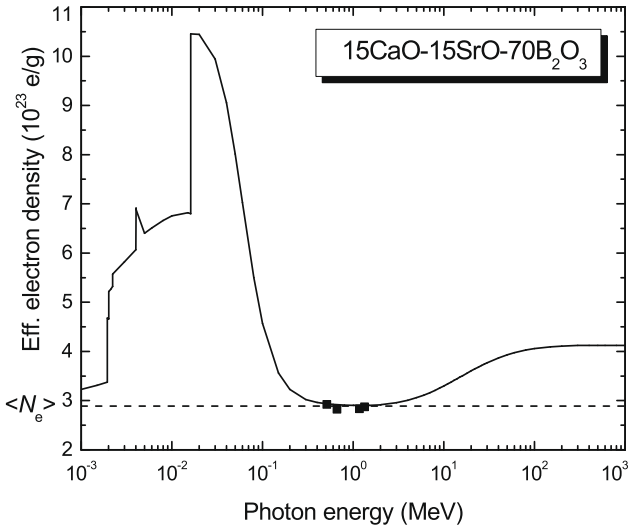


**Fig. 2.** The effective electron density of 15CaO–15SrO–70$B_2O_3$ as a function of photon energy. The squares are experimental data points of Singh et al. [17]. The dashed line indicates the average electron density, $\langle N_e \rangle$.

atomic number mirrors the relative importance of the partial photon interaction processes. Photoelectric absorption is the main interaction process at low energies, whereas incoherent (Compton) scattering dominates at intermediate energies, and pair production at high energies. Coherent (Rayleigh) scattering never plays any significant role, since it occurs at low energies where photoelectric absorption is by far the most important interaction process.

As shown in Fig. 1a, the curve for $Z_{eff}$ has several discontinuous jumps in the low-energy range. The energies of these discontinuities correspond to photoelectric absorption edges of the medium-$Z$ elements: the strontium L edges at 1.940, 2.007, and 2.216 keV, the calcium K edge at 4.038 keV, and the strontium K edge at 16.105 keV (Table 2) (the absorption edges of the low-$Z$ elements boron and oxygen occur at energies <1 keV and are therefore of no importance in the present work). These discontinuities make the concept of the effective atomic number somewhat problematic in the low-energy range ($E < 0.02$ MeV). Above 0.03 MeV, the effective atomic number decreases rapidly with increasing energy in a transition range $0.03 < E < 0.3$ MeV, where the importance of photoelectric absorption decreases and Compton scattering gradually becomes the main interaction process.

Fig. 1a shows that the effective atomic number of 15CaO–15SrO–70$B_2O_3$ is about constant in a wide energy range $0.3 < E < 4$ MeV. At these intermediate energies, Compton scattering is dominating. As we have shown previously [6], the effective atomic number is then given by the mean atomic number of the material. Accordingly, the effective atomic number of 15CaO–15SrO–70$B_2O_3$ is ~8.51 (cf. Table 1, sample #4) at energies $0.3 < E < 4$ MeV.

Fig. 1a also shows that there is another transition range $4 < E < 100$ MeV, where the effective atomic number increases with increasing energy as pair production gradually becomes the main interaction process. Above 100 MeV, pair production is dominating and the effective atomic number is again about constant. For 15CaO–15SrO–70$B_2O_3$, $Z_{eff}$ is about 12.1 in the high-energy range.

As discussed above, the effective atomic number at intermediate energies is close to the mean atomic number of the material. In the low- and high-energy regions, however, $Z_{eff}$ is a weighted mean, where the element with the highest atomic number has the greatest weight. The weighted mean will therefore be larger than the simple mean. Thus, the minimum value $Z_{eff,min}$ is found at intermediate energies ($0.3 < E < 4$ MeV) and approximately

**Table 2**
Photon energies (in keV) of absorption edges above 1 keV.

| Element | Z | M5 | M4 | M3 | M2 | M1 | L3 | L2 | L1 | K |
|---|---|---|---|---|---|---|---|---|---|---|
| Ca | 20 | – | – | – | – | – | – | – | – | 4.038 |
| Sr | 38 | – | – | – | – | – | 1.940 | 2.007 | 2.216 | 16.105 |
| Pb | 82 | 2.484 | 2.586 | 3.066 | 3.554 | 3.851 | 13.035 | 15.200 | 15.861 | 88.005 |
| Bi | 83 | 2.580 | 2.688 | 3.177 | 3.696 | 3.999 | 13.419 | 15.711 | 16.388 | 90.526 |

equal to the mean atomic number, $\langle Z \rangle$. The maximum value $Z_{\text{eff,max}}$ is found at low energies ($E < 0.03$ MeV), where the $Z^4$ dependence of the photoelectric absorption cross-section gives a heavy weight to the highest atomic number of the material. Pair production, which is dominating at high energies ($E > 100$ MeV), has a weaker $Z^2$ dependence and gives less weight to the higher-$Z$ elements than photoelectric absorption. Similar observations have been reported in experimental and theoretical studies of bio-molecules [21–24].

Generally, the effective atomic number for photon energy absorption (Fig. 1b) is varying with energy in the same way as the effective atomic number for photon interaction (Fig. 1a). Significant differences occur in the transition from photoelectric absorption to Compton scattering. The transition range is now $0.05 < E < 0.5$ MeV, i.e. it is shifted to higher energy than for photon interaction discussed above. The physical explanation is that Compton scattering is of less importance for energy absorption than for photon interaction. Accordingly, the region of dominating photoelectric absorption extends to higher energies for energy absorption than for photon interaction. Above about 0.5 MeV the $Z_{\text{eff}}$ curves for photon interaction (Fig. 1a) and energy absorption (Fig. 1b) are practically identical.

The effective electron density, $N_{\text{e,eff}}$, is closely related to the effective atomic number as shown by Eq. (2). Accordingly, the qualitative energy dependence of $N_{\text{e,eff}}$ (Fig. 2) is similar to that of $Z_{\text{eff}}$ (Fig. 1a). It is seen that $N_{\text{e,eff}}$ is about constant at intermediate energies ($0.3 < E < 4$ MeV), where Compton scattering is dominating. As discussed above, the effective atomic number is here equal to the mean atomic number, $\langle Z \rangle$. It then follows from Eqs. (2) and (3) that, at these energies, the effective electron density is identical with the average electron density, $\langle N_e \rangle$, which in the present case is $2.89 \times 10^{23}$ electrons/g.

Fig. 3 shows the effective atomic number as a function of the weight fraction of strontium for some selected energies. It is seen that the relationship is essentially linear for this medium-$Z$ element.

The energy dependence, *ED*, is plotted as a function of photon energy in Fig. 4. It is seen that *ED* has a strong and broad photopeak around 0.04 MeV (note the logarithmic scale for *ED*). It is also seen that *ED* is approximately unity at intermediate energies ($0.3 < E < 4$ MeV), where Compton scattering is the dominating interaction process. Generally, *ED* is varying linearly with $Z_{\text{PEA,eff}}$. This confirms the validity of the general method of estimating *ED* from the effective atomic number in thermoluminescent (TL) dosimetry [25].

### 3.2. Heavy-metal oxide (HMO) glasses

Fig. 5a–c are showing the effective atomic number (for photon interaction) of some PbO and $Bi_2O_3$ based glasses (samples #13, 22, and 29) as a function of photon energy. It is seen that the numerous K-, L-, and M-absorption edges of the high-$Z$ elements Pb and Bi (Table 2) make the low-energy dependence of $Z_{\text{eff}}$ considerably more complicated than for CaO–SrO–$B_2O_3$. Another feature, where the HMO glasses differ from CaO–SrO–$B_2O_3$, is the absence of any extended energy region where $Z_{\text{eff}}$ is about constant and equal to mean atomic number. It is seen that the curve for $Z_{\text{eff}}$ of the HMO glasses has a dip slightly above 1 MeV. However, the minimum value is larger than $\langle Z \rangle$, which would be typical for pure Compton scattering. Thus, we can conclude that Compton scattering is never truly dominating in the HMO glasses.

The comments above are valid also for the effective electron density, $N_{\text{e,eff}}$, of the HMO glasses. Fig. 6 illustrates the case for $60PbO–40B_2O_3$ (sample #13). It is seen that $N_{\text{e,eff}}$ has a dip slightly above 1 MeV, but the minimum value is larger than $\langle N_e \rangle$, which would be typical for pure Compton scattering.

The variation of the effective atomic number with the weight fraction of the heavy element Pb is illustrated in Fig. 7 for the system PbO–$B_2O_3$. In contrast to the Sr based glass (Fig. 3), the relationship is markedly non-linear for the HMO glass.

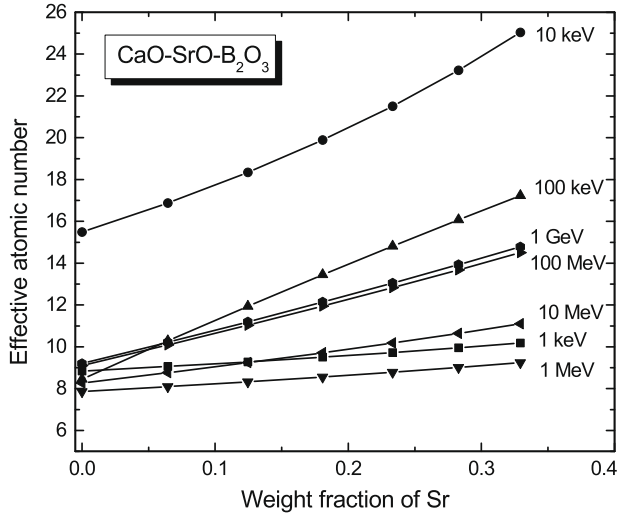


**Fig. 3.** The effective atomic number (photon interaction) of CaO–SrO–$B_2O_3$ as a function of the weight fraction of Sr.

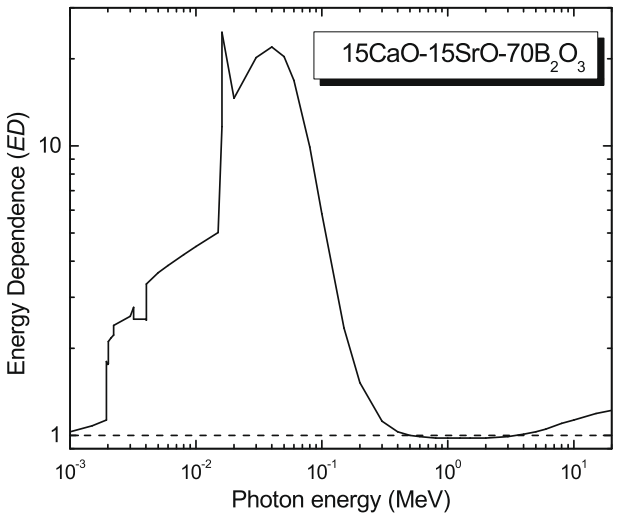


**Fig. 4.** The energy dependence, *ED*, of $15CaO–15SrO–70B_2O_3$ as a function of photon energy. The dashed line indicates *ED* equal to unity.

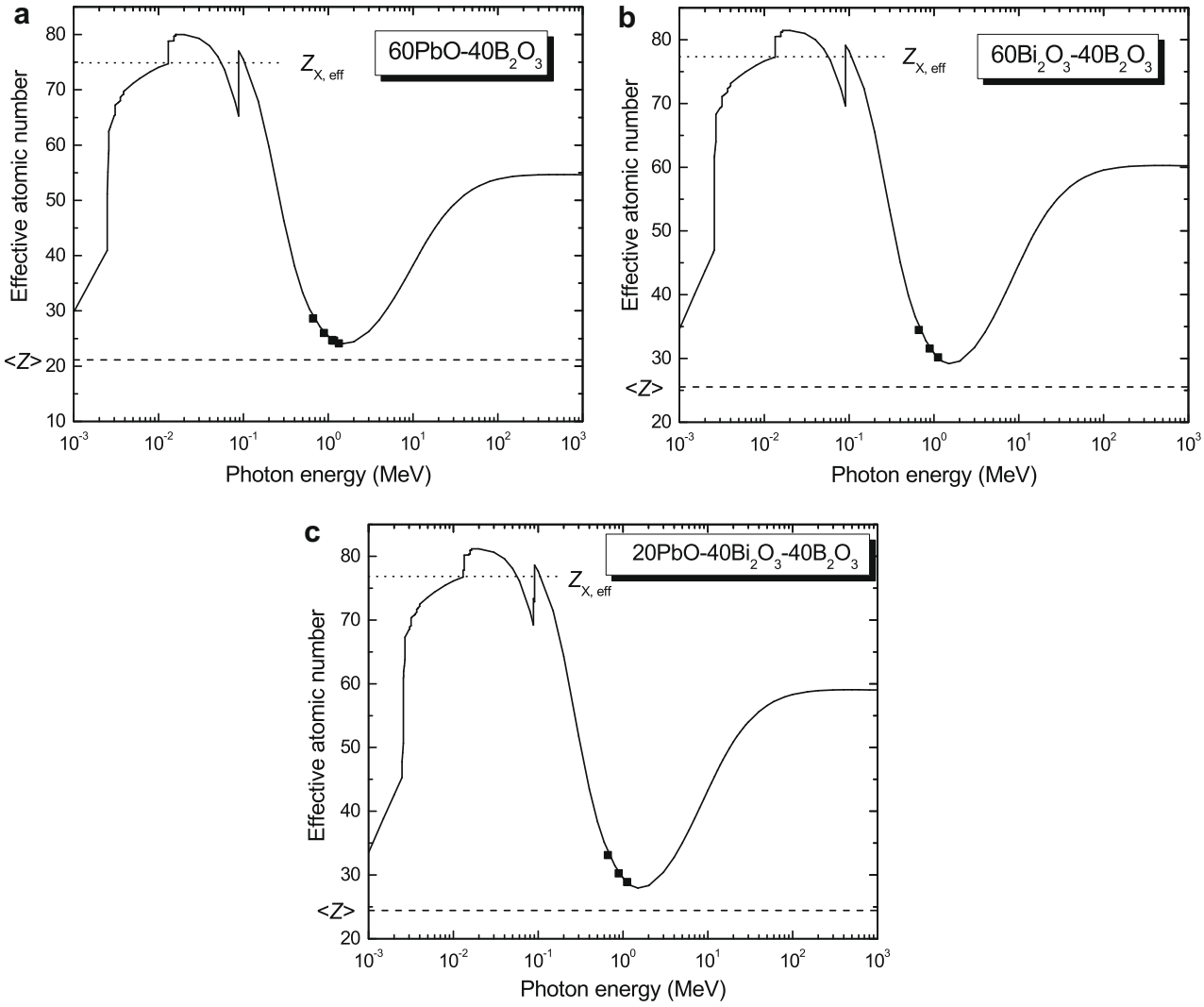


**Fig. 5.** The effective atomic number (photon interaction) of HMO glasses as a function of photon energy. The squares are data points derived from experimental $\mu/\rho$ values of Goswami and Chaudhari [26] and Jayaraman and Rao [27]. The dashed line indicates the mean atomic number, $\langle Z \rangle$, and the dotted line the single-valued effective atomic number, $Z_{X,eff}$, provided by XMuDat. (a) $60PbO–40B_2O_3$. (b) $60Bi_2O_3–40B_2O_3$. (c) $20PbO–40Bi_2O_3–40B_2O_3$.

The energy dependence, *ED*, of some HMO glasses (samples #13, 22, and 29) is plotted as a function of photon energy in Fig. 8a–c. As in the case of $CaO–SrO–B_2O_3$, there is a broad photopeak at 0.04 MeV. In accordance with the discussion above, there is no extended energy range where *ED* is unity but only a dip at about 2 MeV.

### 3.3. The effective atomic number calculated by XMuDat

As mentioned above, the program XMuDat provides, for a given compound or mixture, a single-valued effective atomic number, $Z_{X,eff}$. It is important to note that Eq. (5), from which $Z_{X,eff}$ is calculated, is based on a parameterization of the photoelectric absorption cross-section. Thus, $Z_{X,eff}$ is an approximation of the effective atomic number at energies where photoelectric absorption is the dominating photon interaction process. Accordingly, $Z_{X,eff}$ is close to the maximum effective atomic number, $(Z_{PI,eff})_{max}$, as seen in Table 1. This point is more clearly demonstrated in Figs. 1a,b and 5a–c by the dotted line, representing $Z_{X,eff}$. It is obvious that $Z_{X,eff}$ is only a rough approximation at low energies where photoelectric absorption is dominating. Moreover, the presence of absorption edges is not taken into account. Users of XMuDat should therefore treat $Z_{X,eff}$ with some caution.

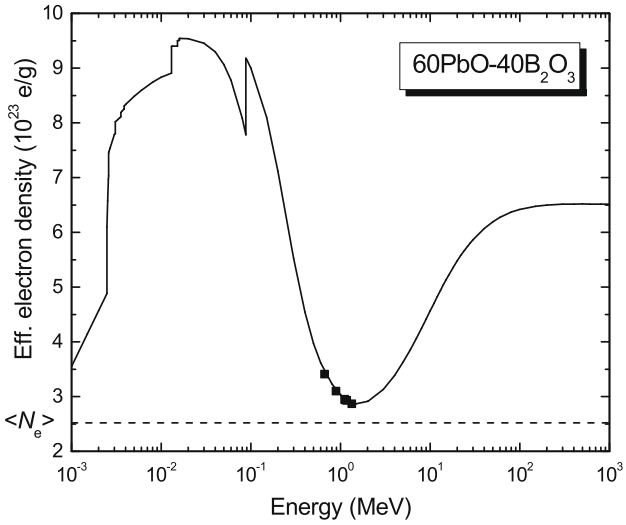


**Fig. 6.** The effective electron density of $60PbO–40B_2O_3$ as a function of photon energy. The squares are data points derived from experimental $\mu/\rho$ values of Goswami and Chaudhari [26] and Jayaraman and Rao [27]. The dashed line indicates the average electron density, $\langle N_e \rangle$.

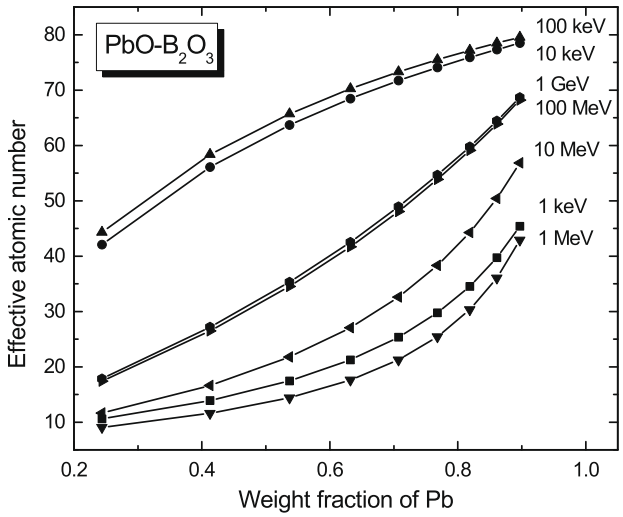


**Fig. 7.** The effective atomic number (photon interaction) of $PbO–B_2O_3$ as a function of the weight fraction of Pb.

As mentioned above, XMuDat also provides an electron density. In fact, XMuDat calculates the average electron density given by Eq. (3). For low- and medium-*Z* materials, the average electron density is identical with the effective electron density at energies where Compton scattering is the dominating photon interaction process.

### 3.4. Comparisons with experiment

Singh et al. [17] have measured the effective atomic number and the effective electron density of $CaO–SrO–B_2O_3$ glasses. Their data points for $15CaO–15SrO–70B_2O_3$ are included in Figs. 1a and 2. The experimental data points for $60PbO–40B_2O_3$, $60Bi_2O_3–40B_2O_3$, and $20PbO–40Bi_2O_3–40B_2O_3$ (Figs. 5a–c), have been derived from mass attenuation coefficients measured by Goswami and Chaudhuri [26] and Jayaraman and Rao [27]. A more detailed comparison between experiment and theory is given in Table 3. There is generally a good agreement between experiment and our calculated curves. It should be mentioned, however, that all experimental work so far has been done at intermediate energies (around 1 MeV) where Compton scattering is the main interaction process. It would be desirable to have experimental data also at other energies. In particular, the transition ranges between photoelectric absorption and Compton scattering, and between Compton scattering and pair production should be interesting.

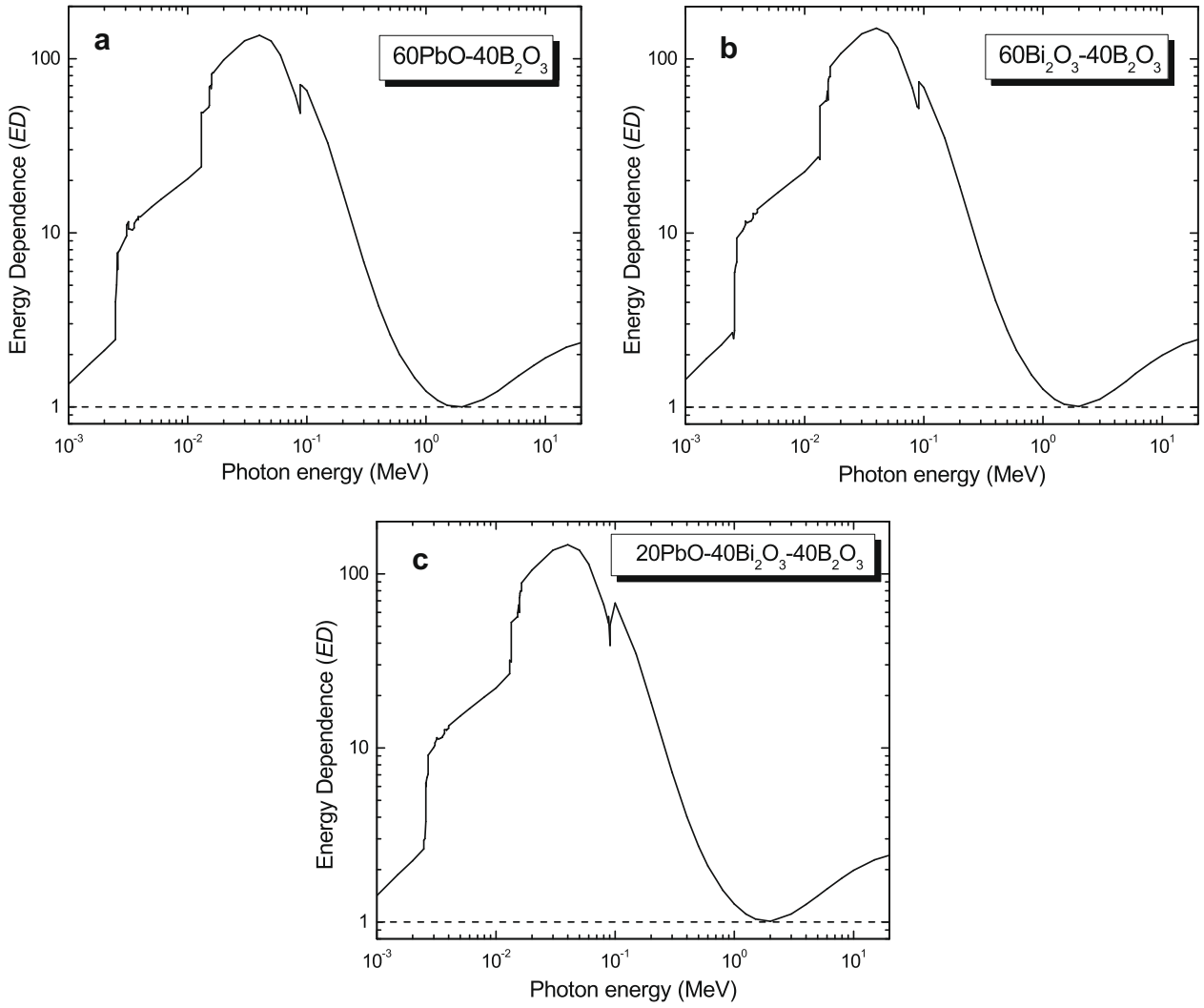


**Fig. 8.** The energy dependence, *ED*, of HMO glasses as a function of photon energy. The dashed line indicates *ED* equal to unity. (a) $60PbO–40B_2O_3$. (b) $60Bi_2O_3–40B_2O_3$. (c) $20PbO–40Bi_2O_3–40B_2O_3$.

**Table 3**
Calculated and experimental values of $Z_{PI,eff}$ for glasses of the present work.

| S.N. | 662 keV | | 889 keV | | 1115 keV | | 1120 keV | | 1173 keV | | 1332 keV | |
|---|---|---|---|---|---|---|---|---|---|---|---|---|
| | a | b | a | b | a | b | a | b | a | b | a | b |
| 2 | 8.59 | 9.07 | – | – | – | – | – | – | 8.76 | 9.01 | 8.77 | 9.00 |
| 3 | 8.39 | 8.83 | – | – | – | – | – | – | 8.57 | 8.78 | 8.62 | 8.77 |
| 4 | 8.27 | 8.59 | – | – | – | – | – | – | 8.39 | 8.55 | 8.46 | 8.55 |
| 5 | 8.07 | 8.35 | – | – | – | – | – | – | 8.21 | 8.32 | 8.26 | 8.32 |
| 6 | 7.85 | 8.11 | – | – | – | – | – | – | 7.98 | 8.10 | 8.04 | 8.08 |
| 8 | 9.60 | 9.66 | 9.15 | 9.18 | 8.93 | 8.97 | 8.94 | 8.96 | 8.94 | 8.93 | 8.86 | 8.87 |
| 9 | 12.66 | 12.79 | 11.76 | 11.83 | 11.32 | 11.39 | 11.35 | 11.38 | 11.33 | 11.32 | 11.17 | 11.19 |
| 10 | 16.03 | 16.24 | 14.69 | 14.79 | 14.02 | 14.12 | 14.06 | 14.11 | 14.02 | 14.01 | 13.78 | 13.82 |
| 11 | 19.77 | 20.06 | 17.99 | 18.13 | 17.08 | 17.21 | 17.14 | 17.20 | 17.08 | 17.06 | 16.75 | 16.80 |
| 12 | 23.95 | 24.31 | 21.73 | 21.91 | 20.60 | 20.76 | 20.67 | 20.74 | 20.58 | 20.56 | 20.17 | 20.24 |
| 13 | 28.63 | 29.06 | 26.02 | 26.23 | 24.67 | 24.85 | 24.75 | 24.83 | 24.62 | 24.62 | 24.13 | 24.22 |
| 14 | 33.92 | 34.42 | 30.98 | 31.23 | 29.44 | 29.63 | 29.53 | 29.61 | 29.36 | 29.37 | 28.80 | 28.90 |
| 15 | 39.95 | 40.51 | 36.79 | 37.06 | 35.10 | 35.30 | 35.19 | 35.27 | 34.98 | 35.00 | 34.37 | 34.48 |
| 16 | 46.88 | 47.49 | 43.68 | 43.96 | 41.93 | 42.12 | 42.02 | 42.09 | 41.75 | 41.80 | 41.12 | 41.25 |
| 17 | 12.14 | 12.28 | 11.32 | 11.39 | – | – | 10.97 | 10.96 | – | – | – | – |
| 18 | 17.14 | 17.42 | 15.67 | 15.79 | – | – | 15.02 | 15.00 | – | – | – | – |
| 19 | 21.85 | 22.24 | 19.86 | 20.02 | – | – | 18.97 | 18.93 | – | – | – | – |
| 20 | 26.30 | 26.78 | 23.90 | 24.10 | – | – | 22.81 | 22.75 | – | – | – | – |
| 21 | 30.50 | 31.06 | 27.79 | 28.02 | – | – | 26.54 | 26.47 | – | – | – | – |
| 22 | 34.48 | 35.10 | 31.55 | 31.80 | – | – | 30.18 | 30.10 | – | – | – | – |
| 23 | 38.26 | 38.93 | 35.17 | 35.44 | – | – | 33.72 | 33.62 | – | – | – | – |
| 24 | 41.84 | 42.55 | 38.68 | 38.96 | – | – | 37.17 | 37.06 | – | – | – | – |
| 25 | 45.24 | 45.99 | 42.07 | 42.35 | – | – | 40.53 | 40.41 | – | – | – | – |
| 26 | 13.57 | 13.75 | 12.56 | 12.64 | – | – | 12.11 | 12.11 | – | – | – | – |
| 27 | 20.21 | 20.54 | 18.38 | 18.53 | – | – | 17.56 | 17.55 | – | – | – | – |
| 28 | 26.72 | 27.19 | 24.27 | 24.48 | – | – | 23.15 | 23.12 | – | – | – | – |
| 29 | 33.11 | 33.69 | 30.24 | 30.48 | – | – | 28.89 | 28.84 | – | – | – | – |
| 30 | 39.39 | 40.05 | 36.27 | 36.54 | – | – | 34.77 | 34.71 | – | – | – | – |
| 31 | 45.55 | 46.27 | 42.38 | 42.66 | – | – | 40.81 | 40.73 | – | – | – | – |

[a]Experimental $Z_{PI,eff}$ values from Ref. [17], and values derived from experimental values of $\mu\rho$ from Refs. [26,27].
[b]Calculated values of the present work.

### 3.5. Accuracy of calculations

Eq. (1) shows that the accuracy of the calculated effective numbers is solely determined by the accuracy of the elemental mass attenuation coefficients, $(\mu/\rho)_i$. Boone and Chavez [28] concluded, in a comparison of X-ray cross-sections for diagnostic and therapeutic medical physics, that the global average differences over the photon energy region from 10 keV to 1 MeV and for elements $Z = 10$–80 is 1.4% for the mass attenuation coefficients and 2.6% for the mass energy-absorption coefficients. Similarly, Hubbell [29] noticed that the envelope of uncertainty of $\mu/\rho$ is of the order of 1–2% in the energy range of most interest in medical and biological applications, from 5 keV to a few MeV. Discrepancies of 25–50% are known to occur in the energy region 1–4 keV. However, those low energies are of little interest in gamma ray shielding. Thus, we conclude that our calculated $Z_{eff}$ values are accurate to within a few percentages at energies above 5 keV.

### 3.6. Comparisons with standard gamma ray shielding materials

The present glasses have been compared with standard radiation-shielding concretes [30] in terms of density, effective atomic number, mass attenuation coefficient and half value layer (HVL). It is found that the mass attenuation coefficient of the present glasses is larger than for ordinary concrete. Moreover, the HVL values of the present HMO glasses (with a mole fraction of heavy-metal oxides larger than 0.30) are smaller than for steel–magnetite concrete.

Bismuth is a good substitute for lead in order to improve the radiation-shielding properties. Thus, the $Bi_2O_3$–$B_2O_3$ glasses have higher effective atomic numbers and stronger absorption of gamma rays than the corresponding PbO–$B_2O_3$ glasses. We conclude that $Bi_2O_3$–$B_2O_3$ have better radiation shielding properties than standard shielding concrete and comparable glasses. Moreover, $Bi_2O_3$–$B_2O_3$ can withstand higher temperatures.

## 4. Conclusions

- For low- and medium-$Z$ glasses, Compton scattering is the totally dominating photon interaction process in a wide energy range around 1 MeV, typically $0.3 < E < 4$ MeV. In this energy region, the effective atomic number, $Z_{eff}$, is about constant and equal to the mean atomic number, $\langle Z\rangle$, of the material. Moreover, at these energies the effective electron density, $N_{e,eff}$, is approximately equal to the average electron density, $\langle N_e\rangle$.
- In contrast, there is no energy region where Compton scattering is truly dominating for the heavy-metal oxide glasses. The effective atomic number has a dip at about 1 MeV, but it does not reach the low value $\langle Z\rangle$ typical for pure Compton scattering.
- Heavy-metal oxide (HMO) glasses containing PbO and/or $Bi_2O_3$ are promising gamma ray shielding materials due to their high effective atomic number and strong absorption of gamma rays. HMO glasses compare well with concrete and other standard shielding materials with the additional advantage of being transparent to visible light.
- Bismuth is a good substitute for lead in order to improve the radiation-shielding properties. Moreover, $Bi_2O_3$–$B_2O_3$ glasses can be used at high temperatures.
- The single-valued effective atomic number provided by XMuDat is approximately valid at low energies where photoelectric absorption is dominating.
- The electron density provided by XMuDat is identical with the average electron density of the material.
- Our calculated $Z_{eff}$ values are accurate to within a few percentages at photon energies above 5 keV.

## References


[1] S. Anilkumar, A.K. Deepa, K. Narayani, A.K. Rekha, P.V. Achuthan, G. Krishnamachari, D.N. Sharma, J. Radioanal. Nucl. Chem. 274 (2007) 164.
[2] D.F. Jackson, D.J. Hawkes, Phys. Rep. 70 (1981) 169.
[3] L. Gerward, N. Guilbert, K.B. Jensen, H. Levring, Radiat. Phys. Chem. 60 (2001) 23.
[4] L. Gerward, N. Guilbert, K.B. Jensen, H. Levring, Radiat. Phys. Chem. 71 (2004) 653.
[5] M.J. Berger, J.H. Hubbell, XCOM: photon cross sections database, Web version 1.2, 1999, Available from: <http://physics.nist.gov/xcom>, originally published as NBSIR 87-3597: XCOM: Photon Cross Sections on a Personal Computer, Washington, DC, 1987.
[6] S.R. Manohara, S.M. Hanagodimath, K.S. Thind, L. Gerward, Nucl. Instrum. Methods B 266 (2008) 3906.
[7] A. Khanna, S.S. Bhatti, K.J. Singh, K.S. Thind, Nucl. Instrum. Methods B 114 (1996) 217.
[8] N. Singh, K.J. Singh, K. Singh, H. Singh, Nucl. Instrum. Methods B 225 (2004) 305.
[9] H. Singh, K. Singh, G. Sharma, R. Nathuram, H.S. Sahota, Nucl. Sci. Eng. 142 (2002) 342.
[10] K. Singh, H. Singh, G. Sharma, R. Nathuram, A. Khanna, R. Kumar, S.S. Bhatti, H.S. Sahota, Nucl. Instrum. Methods B 194 (2002) 1.
[11] H. Gill, G. Kaur, K. Singh, V. Kumar, J. Singh, Radiat. Phys. Chem. 51 (1998) 671.
[12] S.E. Van Kirk, S.W. Martin, J. Am. Ceram. Soc. 75 (1992) 1028.
[13] N. Ford, D. Holland, Glass. Technol. 28 (1987) 106.
[14] N. Singh, K.J. Singh, K. Singh, H. Singh, Radiat. Meas. 41 (2006) 84.
[15] H. Singh, K. Singh, G. Sharma, L. Gerward, R. Nathuram, B.S. Lark, H.S. Sahota, A. Khanna, Phys. Chem. Glasses 44 (2003) 5.
[16] H. Singh, K. Singh, L. Gerward, K. Singh, H.S. Sahota, R. Nathuram, Nucl. Instrum. Methods B 207 (2003) 257.
[17] K. Singh, H. Singh, G. Sharma, L. Gerward, A. Khanna, R. Kumar, R. Nathuram, H.S. Sahota, Radiat. Phys. Chem. 72 (2005) 225.
[18] R. Nowotny, XMuDat: Photon Attenuation Data on PC (Version.1.0.1), IAEA-NDS-195, Vienna, 1998.
[19] J.H. Hubbell, S.M. Seltzer, Tables of X-ray Mass Attenuation Coefficients and Mass Energy-absorption Coefficients 1 keV to 20 MeV for Elements $Z = 1$ to 92 and 48 Additional Substances of Dosimetric Interest, NISTIR-5632, National Institute of Standards and Technology, Gaithersburg, 1995.
[20] F.H. Attix, Health Phys. 15 (1968) 49.
[21] V. Manjunathaguru, T.K. Umesh, J. Phys. B: At. Mol. Opt. Phys. 39 (2006) 3969.
[22] V. Manjunathaguru, T.K. Umesh, J. Phys, J. Phys. B: At. Mol. Opt. Phys. 40 (2007) 3707.
[23] S.R. Manohara, S.M. Hanagodimath, L. Gerward, Med. Phys. 35 (2008) 388.
[24] S.R. Manohara, S.M. Hanagodimath, L. Gerward, Appl. Radiat. Isot., in press.
[25] K. Becker, Solid State Radiation Dosimetry, CRC Press, Boca Raton, 1973.
[26] B. Goswami, N. Chaudhari, Phys. Rev. A 7 (1973) 1912.
[27] R. Jayaraman, V.V. Rao, Appl. Radiat. Isot. 43 (1992) 1139.
[28] J.M. Boone, A.E. Chavez, Med. Phys. 23 (1996) 1997.
[29] J.H. Hubbell, Phys. Med. Biol. 44 (1999) R1.
[30] I.I. Bashter, Ann. Nucl. Energy 24 (1997) 1389.